jbc The Journal of Biological Chemistry
AFFINITY SITES
ASBMB American Society for Biochemistry and Molecular Biology

Cell Biology:

Histone deacetylase 3 unconventional splicing mediates endothelial-to-mesenchymal transition through transforming growth factor β2

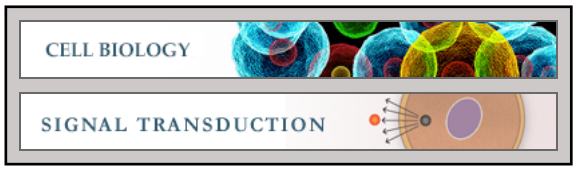

Lingfang Zeng, Gang Wang, Dario Ummarino, Andriani Margariti, Qihe Xu, Qingzhong Xiao, Wen Wang, Zhongyi Zhang, Xiaoke Yin, Manuel Mayr, Gillian Cockerill, Julie Yi-Shuan Li, Shu Chien, Yanhua Hu and Qingbo Xu

J. Biol. Chem. *published online September 17, 2013*

Access the most updated version of this article at doi: 10.1074/jbc.M113.463745

Find articles, minireviews, Reflections and Classics on similar topics on the JBC Affinity Sites.

Alerts:
- When this article is cited
- When a correction for this article is posted

Click here to choose from all of JBC's e-mail alerts

This article cites 0 references, 0 of which can be accessed free at
http://www.jbc.org/content/early/2013/09/17/jbc.M113.463745.full.html#ref-list-1

Downloaded from http://www.jbc.org/ at KING'S COLLEGE LONDON on October 11, 2013

JBC Papers in Press. Published on September 17, 2013 as Manuscript M113.463745
The latest version is at http://www.jbc.org/cgi/doi/10.1074/jbc.M113.463745

Histone deacetylase 3 unconventional splicing mediates endothelial-to-mesenchymal transition through transforming growth factor beta 2

Running Title: HDAC3 splicing and EndMT

Lingfang Zeng[1], Gang Wang[2], Dario Ummarino[1], Andriana Margariti[1], Qihe Xu[3], Qingzhong Xiao[4], Wen Wang[5], Zhongyi Zhang[1], Xiaoke Yin[1], Manuel Mayr[1], Gillian Cockerill[6], Julie Yi-shuan Li[7], Shu Chien[7], Yanhua Hu[1], Qingbo Xu[1]

[1]Cardiovascular Division, King's College London BHF Centre, London SE5 9NU, UK

[2]Department of Emergency Medicine, the Second Affiliated Hospital, Xi'an Jiaotong University School of Medicine, Shaanxi, PR China

[3]Department of Renal Medicine, King's College London, London SE5 9NU, UK

[4]Clinical Pharmacology, William Harvey Research Institute, Barts and The London School of Medicine and Dentistry, Queen Mary University of London, London EC1M 6BQ, UK

[5]Medical Engineering Division, School of Engineering and Materials Science, Queen Mary University of London, London E1 4NS, UK

[6]Department of Cardiovascular Science, St. George's University of London, London SW17 0RE, UK

[7]Department of Bioengineering and Medicine, University of California at San Diego, La Jolla, CA92093, USA

Zeng L and Wang G contributed equally to this study.

Correspondence to: Dr Lingfang Zeng, Cardiovascular Division, King's College London, 125 Cold harbour Lane, London SE5 9NU, UK. Tel: +44-2078485270; Fax: +44-2078485296; E-mail: lingfang.zeng@kcl.ac.uk

Background: Endothelial-to-mesenchymal transition (EndMT) is involved in embryonic cardiovascular development.

Results: HDAC3 undergoes unconventional splicing during stem cell differentiation, which contributes to EndMT.

Conclusion: HDAC3 unconventional splicing may modulate endothelial cell plasticity.

Significance: Targeting HDAC3 splicing may provide new therapeutic strategies to tackle cardiovascular disease caused by endothelial plasticity.

Summary

Histone deacetylase 3 (HDAC3) plays a critical role in the maintenance of endothelial integrity and other physiological processes. In this study, we demonstrated that HDAC3 undergoes unconventional splicing during stem cell differentiation. Four different splicing variants have been identified, designated as HD3α, β, γ and δ, respectively. HD3α was confirmed in stem cell differentiation by specific antibody against the sequences from intron 12. Immunofluorescence staining indicated that HD3α isoform co-localized with CD31 positive or alpha smooth muscle actin positive cells at different developmental stages of mouse embryos. Over-expression of HD3α reprogrammed human aortic endothelial cells into mesenchymal cells featuring an endothelial-to-mesenchymal transition (EndMT) phenotype. HD3α directly interacts with HDAC3 and Akt1, and selectively activates transforming growth factor β2 (TGFβ2) secretion and cleavage. TGFβ2 functioned as an autocrine and/or paracrine EndMT factor. The HD3α–induced EndMT was both PI3K/Akt and TGFβ2 dependent.

Copyright 2013 by The American Society for Biochemistry and Molecular Biology, Inc.

This study provides the first evidence on the role of HDAC3 splicing in the maintenance of endothelial integrity.

Key words: HDAC3, unconventional splicing, TGFβ2, PI3/Akt, endothelial-to-mesenchymal transition

Introduction

As a key cellular component of the circulatory system, endothelial cells (ECs) play important roles in cardiovascular homeostasis and disease development. In response to local flow patterns and physiological stimuli, ECs can exhibit a wide range of phenotypic variability throughout the cardiovascular system(1). The most remarkable feature is the plasticity of endothelial-to-mesenchymal transition (EndMT), which contributes to embryonic cardio-genesis(2-6), postnatal angiogenesis(7), and pathological processes such as cardiac(8) and renal fibrosis(9), pulmonary hypertension(10), and tumor angiogenesis and metastasis(11,12).

EndMT defines a specific type of cell plasticity. During EndMT, resident ECs delaminate from an organized cell layer and invade the underlying tissue. These cells lose cell-cell junctions due to decreased VE-cadherin, acquire invasive and migratory properties and lose other EC markers such as CD31. On the other hand, these cells gain mesenchymal markers, e.g. fibroblast-specific protein 1(FSP1), N-cadherin and alpha-smooth muscle actin (αSMA)(5,8,10,13,14). EndMT was originally identified in cardiogenesis. A subset of ECs in the endocardium of mouse embryos at 9.5 day post-coitus (dpc) transform into mesenchymal cells that migrate, proliferate and eventually remodel the cardiac cushions into heart valve leaflets and septa for a partitioned heart(2,3). Recent reports revealed that EndMT accounts for up to 40% cancer-associated fibroblasts, which is the main source of host-derived vascular endothelial cell growth factor (VEGF)(11). Several signaling pathways are reported to be involved in EndMT, such as transforming growth factor beta (TGF-β) binding, Notch and Akt1 activation(5,8,15). A very recent study showed that EndMT is also involved in neointima formation(16). However, the mechanism of EndMT is still poorly understood.

Histone deacetylases (HDACs) modulate chromatin structure through regulating the acetylation status of histone tails, functioning as transcriptional co-repressors(17,18). Recent studies showed that HDACs can also modulate transcription factor activity, increase gene transcription(19) and interact with cytoskeleton and signal transducers(20-22). There are 18 types of HDACs, classified into four categories. HDAC3 is a member of Class I HDACs(17,23). It is an indispensable gene, removal of which in the germ cell line causes embryonic lethality at an early stage(24). Our previous study indicated that HDAC3 is essential for EC differentiation and integrity maintenance(25-27). In this study, we found that HDAC3 undergoes unconventional splicing during embryonic stem (ES) cell differentiation and development. In addition, over-expression of the splicing isoforms of HDAC3, HD3α, reprogrammed ECs into mesenchymal cells.

Experimental Procedures

Materials

All cell culture media and serum were purchased from Life technologies (Paisley, UK), and cell culture supplements and growth factors were obtained from Sigma-Aldrich (Dorset, UK). Antibodies against HD3α and β were developed by Genescript (Piscataway, USA) in rabbits with peptide PQGDTILTSPQNDL. The same peptide was used as blocking peptide to test the specificity of anti-HD3α/β antibody. Antibodies against CD31 (sc-1506), N-Cad (sc-6461), VE-Cad (sc-9989), GAPDH (sc-25778), Akt1/2 (sc-8312), pAktS473 (sc-7985R), VEGF (sc-507), Snail2 (sc-15391), Smad3

(sc-101154) and CD9 (sc-13118) were purchased from Santa Cruz Biotech (Heidelberg, Germany), antibodies against Flag (F2426, F1804 and F7425), HA (H6908), αSMA (A5228), tubulin (T5201), HDAC3 (H3034), Histone H4 (SAB4500306), pSmad2 (SAB4300251) and pSmad3 (SAB4300253) were from Sigma, while antibodies against FSP1 (ab41532), TGFβ1 (ab9758), TGFβ2 (ab10850), PI3K p85 alpha (ab22653) and collagen IV (ab19808) were from Abcam (Cambridge, UK). Rat anti-CD31 (553369) was from BD Biosciences (Oxford, UK). All secondary antibodies were from Dakocytomation (Glostrup, Denmark). All other chemicals were purchased from Sigma.

Cell culture

Mouse embryonic stem cells (ES-D3 cell line, CRL-1934; ATCC, Manassas, USA), human aortic endothelial cells (HAECs) and 293 cells were maintained as described previously(26,28). $Sca1^+$ cells were isolated from collagen IV-differentiated ES cells and maintained in differentiation medium (DM, alpha-MEM supplemented with 10% FBS from Sigma, $5x10^{-5}$Mol/L β-mercaptoethanol, 100u/ml penicillin/streptomycin) for more than 5 passages. As the majority of these $Sca1^+$ cells are ECs, these are therefore designated as esECs and maintained in DM(27). For ES differentiation, the cells were seeded into collagen IV or I-coated flask in DM for 72 hrs, followed by assessments.

Plasmid construction and transient transfection

HDAC3 splicing variants were amplified with primer set from differentiated mouse ES cells and cloned into the KpnI site of pShuttle2-Flag vector as described previously(26), verified by DNA sequencing and designated as HD3α, β, γ and δ, respectively. For ES or esEC differentiation assay, the cells were transfected with $2\mu g/1x10^6$cells of plasmids (pShuttle-Flag vector, pShuttle-Flag-HDAC3 or pShuttle-Flag-HD3α) with the nucleofection kit (Lonza, Surrey, UK) and cultured in collagen IV-coated dishes in DM in the presence of 5ng/ml mouse VEGF (Sigma) or 20ng/ml rat platelet derived growth factor-BB (PDGF-BB) (Sigma) for 72 hrs. For co-immunoprecipitation, 293 cells were co-transfected with pShuttle-Flag-HD3α, β, γ, δ/pShuttle-HA-HDAC3 or pShuttle-Flag-HD3α, β, γ, δ/pShuttle-HA-Akt1/2 with nucleofection kit at $2\mu g/1x10^6$cells and cultured for 24 hrs.

Adenoviral gene transfer

Ad-HD3α viral vector was created from pShuttle2-Flag-HD3α plasmid, and the resulting adenoviral particles were amplified using Adenoviral expression system (Clontech, Takara Biosciences, St Germaine-en-laye, France) and the manufacturer's protocol. For adenoviral gene transfer, HAECs were incubated with Ad-null or Ad-HD3α virus at the multiplicity of infection (MOI) indicated for 6 hrs. After the removal of virus solution, the cells were cultured in human endothelial serum free medium (SFM, Life technologies) for 24-48hr, or in M199 medium supplemented with 1% FBS for 5 days or in M199 medium supplemented with 5ng/ml insulin for 24hr. For inhibitor or neutralization antibody assays, inhibitors (concentration indicated in figure legends) and neutralization antibody (0.2μg/ml) were included in the whole infection and incubation process. DMSO (same volume) and IgG (0.2μg/ml) were included as vehicle and negative control, respectively.

HD3α/β-GFP transgenic vector construction

HDAC3 DNA fragment covering exon 4 to exon 15 was amplified by PCR from genomic DNA and inserted into pLoxPneo vector. GFP coding sequences were inserted into the open reading frame of HD3α and β within intron-12 upstream the stop codon, while a LoxP-Neo-LoxP cassette was inserted into

intron-12 downstream of the stop codon, creating the pLoxPneo-HD3α/β-GFPkin plasmid. ES-D3 cells were transfected with this plasmid. The positive transfection clones were selected with G418, while the recombinant clones were further selected with Gaciclovir. The positive recombinant clones were then transfected with pCMV-Cre210 plasmid (Addgene, Cambridge, MA) to remove the loxP-Neo-LoxP cassette. The positive HD3α/β-GFP stable cell clones were verified by PCR with primer sets flanking the GFP insertion and LoxP site, respectively. For GFP observation, HD3α/β-GFP transfected ES cells were cultured in Collagen I-coated dishes in DM for 3 days and observed under inverted phase and fluorescence microscopes. Images were taken and processed by Photoshop software.

Indirect Immunofluorescence staining

Cryo-sections (5μm) from mouse embryos at 10.5dpc and 12.5dpc stages or chamber slides of cell culture were fixed with methanol at room temperature for 15 minutes, permeabilized with 0.1% Triton X-100/PBS for 15 minutes, blocked with normal donkey serum (1:20 dilution in PBS) for one hour, incubated with primary antibodies (diluted in blocking serum) and Alexa Fluor®546/488 conjugated secondary antibodies from donkey (Dako) at 37ºC for 1hr and 30min, respectively. Nuclei were counterstained with DAPI. To assess the specificity of HD3α antibody, 10μg/ml of HD3α antibody was incubated with 10μg/ml of the HD3α peptide (used to raise the antibody) at 37ºC for 1 hour prior to primary antibody incubation. Images were obtained with Leica SP5 confocal microscope and LASAF software (Leica, Germany) at 37ºC and processed by Adobe Photoshop software.

Mouse embryonic and adult organ tissues

Pregnant C57BL/6J female mice were sacrificed, and the whole embryos at 8.5dpc, 10.5dpc, 13.5dpc, 15.5dpc, 17.5dpc, 19.5dpc and new born mice at day 1 were harvested for RNA extraction. In the mean time, different organ tissues were harvested from the female mice for RNA extraction. All animal experiments in this study were performed according to protocols approved by the Institutional Committee for Use and Care of Laboratory Animals.

Quantitative RT-PCR assay

Cellular total RNA was isolated using RNeasy kit (Qiagen, Manchester, UK) based on manufacturer's protocol. One μg RNA was reversely transcribed into cDNA with ImproRT system (Promega, Southampton, UK) using random primer, and 10ng cDNA (relative to RNA amount) was used in qPCR with SYBRgreen kit (Life technologies) to analyze the expression of mouse HDAC3 (5'-tatggctgagacaccagagtg-3' and 5'-atctggtcc agatactgggtgag-3'), VE-Cad (5'-atctgtgccaga gatgtcagc-3' and 5'-gaatgtgtactgctggtagac-3'), and SM22 (5'-catgagccgagaa gtgcactc-3' and 5'-ctaa gcaggatgctgcagctc-3'); human TGFβ1 (5'-atcctgcatctggtcacggtc-3' and 5'-cttggcgta gtactcttcgtc-3'), TGFβ2 (5'-aagactatcgacatgga gctg-3' and 5'-gtaccgcttctcggagctctg-3'), TGFβ3(5'-gcacaacgaactggctgtctg-3' and 5'-aa cagccactcacgcacagtg-3'), αSMA (5'-agccaagc actgtcaggaat-3' and 5'-caccatcacccccctgatgtc -3') and HD3α (5'-tatggctga gacaccagagtg-3' and 5'-ttgactcatagcctagtcctg-3'). β-actin (5'-ca caactgggacgacatggag-3' and 5'-ttcatgaggtagt cagtctgg-3') was included as internal control.

Immunoprecipitation and Immunoblotting

Cells were lysed by incubation with IP-A buffer [0.02mol/L Tris-HCl, pH7.5, 0.12mol/L NaCl, $1x10^{-3}$mol/L EDTA, 1% Triton X-100 plus protease inhibitors (Roche, Welwyn Garden City, UK)] on ice for 45 min, followed by protein concentration assessment with Bradford reagent (Bio-Rad, Hertfordshire, UK). One mg of cell lysate was mixed with 2 volume of IP-B buffer (IP-A without Triton X-100), pre-cleared with 2μg normal IgG and 10μl Easyview Protein-G agarose beads

(Sigma), and then incubated with 2μg anti-HA or anti-Flag antibody and 10μl Easyview Protein-G agarose beads. The immune-precipitates were separated by SDS-PAGE and detected by Western blot analysis. Fifty μg of cell lysate was included as input control. Immunoblotting was performed as a standard procedure described elsewhere.

Cellular fractionation

HAECs were collected by scraping in 400μl/75ml-flask of hypotension buffer (0.01mol/L Tris-Cl pH7.5, 0.01mol/L KCl plus protease inhibitors) and incubated on ice with vortexing every 5 min for 15 min. Twenty-five μl of 10% NP-40 was added and vortexed at 200rpm for 10 sec. Nuclei were spun down at 16,100g at 4ºC for 10 sec. The supernatant was recovered as cytosol fraction. The nuclei were washed once with PBS, resuspended in 70μl of hypotension buffer containing 0.625% NP-40, and sonicated for 6 sec. Nuclear extract was recovered from the supernatant by spinning at 16,100g at 4ºC for 5 min. Protein concentration was assessed with BioRad reagent. Twenty-five μg of proteins were applied to Western blot analysis.

Analysis of secreted proteins

HAECs were infected with Ad-null or Ad-HD3α at 10MOI in the absence or presence of inhibitors for 6hr in complete growth medium, followed by washing with serum free M199 medium for 3 times and incubation with M199 medium supplemented with 5ng/ml insulin for 24hr. Conditioned medium was collected and the cell debris was removed by centrifugation at 4000rpm at 4ºC for 5min. The supernatant was recovered and subjected to exosomes isolation and whole medium concentration, respectively. For exosomes isolation, 1ml of the supernatant was mixed with 500μl of total exosomes isolation reagents (Life technologies) and incubated on a rotator at 4ºC for 24hr, followed by spinning at 16,100xg at 4ºC for 1hr. The pellet was resuspended in 25μl of 1x SDS loading buffer (0.02mol/L Tris-HCl pH8.9, 2%SDS, 10% glycerol, 0.5% 2-mercaptoethanol, 0.025% Bromophenol Blue). For total medium concentration, 500μl of the supernatant was applied to an Amicon Ultra-0.5 ultracel-3 membrane unit (Millipore, Watford, UK) and centrifuged at 16,100xg at 4ºC for 15min. This procedure was repeated until 5ml of the supernatant was concentrated to 100μl, which was mixed with 25μl of 5xSDS loading buffer. Twenty five μl of exosomes or concentration sample was applied to SDS-PAGE and Western blot analysis.

SiRNA transfection assay

HAECs were seeded in gelatin-coated 75ml flasks at 50% confluence 24hr before transfection and washed three times with PBS and incubated with both serum and antibiotics free M199 medium 1hr prior to transfection. Upon transfection, 60μl of $1x10^{-5}$mol/L PI3K p85 siRNA (sc-39126, Santa Cruz Biotechnology Inc), Akt1siRNA (sc-29196) or control siRNA (sc-37007) was diluted into 800μl M199 and incubated with pre-diluted lipofectamine RNAiMAX (50μl in 800μl M199 for 5 min, Life technologies) at room temperature for 15 min. The mixture was added to the pre-treated HAECs (6ml/75ml flask of M199 for 1hr) and incubated for 5hr, after which the medium was refreshed with complete growth medium. Forty eight hour post-transfection, the cells were infected with Ad-null or Ad-HD3α and cultured for 24hr, followed by incubation in serum free M199 containing 5ng/ml insulin for 24hr. Cell lysates and culture medium were collected for Western blot analysis of αSMA expression and TGFβ2 secretion, respectively.

Statistical analysis Data expressed as the mean±SEM were analyzed with a two-tailed student's *t*-test for two-groups or pair-wise comparisons or ANOVA for more than one comparison. A value of $p<0.05$ was considered

to be significant.

Results

HDAC3 undergoes unconventional splicing during stem cell differentiation

Our previous study demonstrated that HDAC3 was essential for EC differentiation(26,27). When cloning mouse HDAC3 cDNA sequence using a primer set 5'-atgaccggtaccgtggcgtatttctac gac-3' and 5'-cacagcaagcttgctgctctaaatctccac-3', we discovered a few smaller electrophoretic bands in differentiated embryonic stem (DES) cell samples (Figure 1A). Similar bands were also found in samples from mouse embryos (Figure 1B) and adult tissues (Figure 1C). To verify the nature of these bands, all the bands were isolated and sequenced (Genebank Accession, JN651901-JN651904). Interestingly, the bands appeared to be isoforms spliced in an unconventional way. Four different isoforms have been identified, and designated as HD3α, β, γ and δ (Figure 1D). In HD3α, β and δ, the intron-12 was kept as an additional exon, in which part of the intron sequence was incorporated into the open reading frame (ORF) and ended within the intron (Genebank Accession, JN651901, JN651902 and JN651904). HD3α and HD3β have the same ORF and the only difference is that HD3β loses sequence from exon9 and 10. The ORF of HD3δ downstream exon 3 is totally different from that of HD3α and HD3β. Though all three isoforms contain sequences from intron 12, the C-terminal of HD3δ is different from that of HD3α and HD3β . In addition, recombination appears to be present between exon-3 and -9 for HD3α, between exon-3 and -10 for HD3β and HD3γ, and between exon-3 and intron-12 for HD3δ. All four isoforms share the far N-terminal domain as full length HDAC3, and possess specific C-terminal domain derived from intron-12, except HD3γ. Flag-tag expression of the isoforms in 293 cells revealed the expected protein bands (Figure 1E). To verify that these isoforms were not artifacts derived from RT-PCR, an HDAC3 gene construct was created (pLoxPneo-HD3α/β-GFPkin), in which a GFP coding sequence was inserted into the intron-12 within the ORF of HD3α/β upstream of the stop codon. The construct was transfected into mouse ES cells, and selected sequentially with geneticin G-418 and Gaciclovir. The HD3α/β-GFP knock-in ES cell line was eventually established via removal of the LoxP-Neo-LoxP cassette using pCMV-Cre transfection. Normally, the intron-12 is removed through conventional splicing, so GFP is absent. Although HD3α/β-GFP knock-in ES cells did not yield GFP positive cells in ES culture medium, when these cells were cultured in differentiation medium for 3 days, a portion of the cell population became GFP positive cells (Figure 1F), suggesting that the intron-12 was kept as an additional exon and the intron sequence was incorporated into the ORF. These results suggest that HDAC3 naturally undergoes unconventional splicing during stem cell differentiation, as far as the HD3α/β isoforms are concerned. As the ORF is different, HD3δ can't give rise to GFP. To distinguish HD3α/β isoforms, we raised antibody in rabbit against peptide PQGDTILTSPQNDL from intron-12 (Genebank Accession, JN651901 and JN651902) and performed Western blot on differentiated ES cell samples. A band corresponding to HD3α was detected in DES cells but not in undifferentiated ES cells (Figure 1G left), which disappeared when the antibody was pre-incubated with the blocking peptide (Figure 1G right), suggesting that the antibody is specific. The intensity of this HD3α band was slightly changed in PDGF, TGFβ1 or VEGF treated DES cells. No band corresponding to HD3β was detected (Figure 1G, left). As HD3α is the main isoform, the following study will only focus on HD3α.

As HDAC3 is essential for EC

differentiation(26), we tested whether the splicing event will affect such process by introducing HDAC3 and HD3α into DES cells and esECs(27) via plasmid transfection, followed by quantitative RT-PCR analysis of VE-cadherin (VE-Cad) and SM22 gene expression. As expected, over-expression of HDAC3 increased VE-Cad expression in both ES cells (Figure 1H, left) and esECs (Figure 1I, left) with VEGF having a synergistic effect. HD3α had no effect on VE-Cad or SM22 gene expression in ES cells (Figure 1H). In esECs, however, HD3α decreased VE-Cad (Figure 1I, left) while increased SM22 (Figure 1I, right) expression, especially under PDGF treatment. These results suggest that HD3α may promote ECs trans-differentiation into mesenchymal cells.

HDAC3 splicing may play a role in embryonic development

As described in Figure 1B, spliced HDAC3 bands could be detected in mouse embryos by routine RT-PCR, it is worth investigating whether such splicing event was involved in mouse embryonic development. Mouse embryos were harvested at 10.5dpc and 12.5dpc, respectively. Cryo-sections were made to include the two developmental stages of the vasculogenesis, which starts from endothelial tube formation (Figure 2A) and ends with smooth muscle cell localization (Figure 2B). Immunofluorescence staining with anti-HD3α revealed that HD3α emerged in the CD31 positive endothelial cells during 10.5dpc stage when vasculogenesis begins (Figure 2Ab&c). At 12.5dpc, there is no colocalization of CD31 and HD3a (Figure 2Ba). However, HD3α was found to co-localize with αSMA positive smooth muscle cells (Figure 2Bb&c). Pre-incubation with the blocking peptide abolished HD3α staining (Figure 2Aa), confirming the specificity of anti-HD3α antibody. These results indicate that HD3α is involved in the embryonic vasculogenesis and may be a key regulator in the determination of vascular progenitor cells.

Over-expression of HD3α induces EndMT via PI3K-Akt and TGFβ signal pathways

To confirm whether HD3α is involved in EndMT, the effect of over-expression of HD3α in mature endothelial cell was investigated. Human aortic endothelial cells (HAECs) were infected with Ad-HD3α virus followed by incubation with serum free culture medium or M199 medium supplemented with 1% FBS. 24hr post infection, cell growth rate decreased and some cells underwent morphology change (Figure 3A). Western blot analysis revealed that over-expression of HD3α decreased the EC marker CD31 while increased mesenchymal markers such as N-cadherin (N-cad), αSMA, VEGF and EndMT transcription factor Snail2 in a dose-dependent manner (Figure 3B). Immunofluorescence staining confirmed the EndMT phenotype as revealed by the decrease or redistribution of VE-Cad and occurrence of αSMA in the Ad-HD3α-infected and adjacent cells (Figure 3C). These results suggest that over-expression of HD3α can induce EndMT.

Multiple signal pathways have been reported to be involved in EndMT process, such as TGFβ, PI3K/Akt, MAP kinase, p38, JNK, and RhoA, etc(8,15,29-33). To identify which signal pathway is involved in HD3α–induced EndMT, specific inhibitors LY294002 (PI3K/Akt), PD98059 (MAP kinase), SB202190 (p38), SB431542 (TGFβ), SP60005 (JNK), Y27631 (RhoA) were tested. As shown in Figure 3D, both LY294002 and SB431542 abolished Ad-HD3α-induced αSMA expression in HAECs, while the other inhibitors did not. The inhibitory effect of LY294002 and SB431542 was further confirmed by immunofluorescence staining with anti-VE-Cad (red) and anti-αSMA (green) antibodies (Figure 3E). These experiments suggest that both PI3K/Akt and TGFβ signal pathways are required by HD3α in driving

EndMT.

HD3α induces TGFβ2 activation

TGFβ signalling pathway plays a critical role in EndMT(34). The above study has demonstrated that this pathway is also required by HD3α–induced EndMT. To investigate how HD3α drives EndMT through TGFβ signal pathway, the activation of this pathway was first assessed in Ad-HD3α–infected cells. As shown in Figure 4A, over-expression of HD3α induced Smad2/3 phosphorylation and nuclear translocation and increased Snail2 expression and nuclear translocation. The majority of HD3α itself is located in the cytosol, with only a small portion is located in the nuclear fraction. Further experiments indicated that exogenous TGFβ1 and 2 could induce EndMT, but only TGFβ1 had additive effect on HD3α–induced EndMT (Figure 4B). In the presence of TGFβ1, over-expression of HD3α induced a huge accumulation of phosphor-Smad2 in the nuclei, while the majority of HD3α is located on the nuclear envelop (Figure 4C). These experiments suggest that HD3α drives EndMT through activating Smad2/3 phosphorylation and nuclear translocation.

In the TGFβ signaling axis, TGFβs bind to TGFβ receptor-II, which recruits and phosphorylates TGFβ receptor-I (ALK5). The latter activates Smad2/3 phosphorylation and nuclear translocation (35). As described above (Figure 3D & 3E), ALK5 is essential for HD3α–induced EndMT. Furthermore, adjacent cells next to Ad-HD3α–infected cells also express αSMA (Figure 3C). It is reasonable to assume that HD3α induces the secretion and/or activation of TGFβs, which in turn activate ALK5 in an autocrine and paracrine manner. To test this, we first detected TGFβ1, 2 and 3 mRNA levels by quantitative RT-PCR. Over-expression of HD3α did not seem to affect these gene expression at mRNA levels (Figure 4D). Interestingly, there was also only slight increase at αSMA mRNA level (Figure 4D). Increase of αSMA protein may be mediated by translational regulation. Western blot analysis showed that over-expression of HD3α had no significant effect on TGFβ1 and TGFβ2 protein levels in cell lysate as well, although Smad2 phosphorylation was significantly increased (Figure 4E). However, the analysis of the secreted proteins in conditioned medium indicated that over-expression of HD3α significantly increased TGFβ2 activation via cleavage as revealed by the occurrence of the small electrophoretic band (Figure 4F and 4G). PI3K-Akt inhibitor, LY294002, increased TGFβ1 and TGFβ2 protein levels in Ad-HD3α–infected cells but abolished Ad-HD3α–induced Smad2 phosphorylation (Figure 4E) and attenuated TGFβ2 activation (Figure 4F and 4G). As expected, ALK5 inhibitor SB431542 abolished HD3α–induced Smad2 phosphorylation (Figure 4E) and the active TGFβ2 was accumulated in Ad-HD3α–infected cell medium (Figure 4F and 4G). TGFβ1 is reported to be secreted by exosomes(36). To test whether the secretion of TGFβ2 is also mediated by exosomes, TGFβ2 was detected in cell lysate, exosomes and whole medium concentrates by Western blot. Exosomes were confirmed by the presence of CD9 protein(37). As expected, higher level of TGFβ1 was detected in exosomes as compared to the medium (Figure 4H). However, the majority of the secreted TGFβ2, either the precursor (50KD band) or active band (13KD, arrow in Figure 4H) locates in the whole medium concentrates but not in exosomes, suggesting that TGFβ2 is secreted by mechanisms other than exosomes. Further experiments revealed that the presence of TGFβ2 neutralization antibody attenuated HD3α–induced Smad2 phosphorylation and αSMA expression (Figure 4I). These results suggest that HD3α induces TGFβ2 protein secretion and activation in a PI3K-Akt

pathway-dependent manner, and that the active TGFβ2 in turn functions as an autocrine and/or paracrine factor to activate downstream signal pathways, leading to EndMT.

HD3α physically interacts with Akt1

PI3K-Akt pathway plays a central role in EMT(38). As described above, our study has demonstrated that an active PI3K-Akt pathway is essential to HD3α–induced TGFβ2 activation and EndMT. The question is how PI3K-Akt cross-talks with HD3α. To test this, Akt phosphorylation was assessed by Western blot following Ad-HD3α infection. As shown in Figure 5A, over-expression of HD3α did not cause a significant up-regulation of Akt phosphorylation, suggesting that HD3α itself does not activate PI3K-Akt pathway. Our previous study has shown that HDAC3 could associate with Akt1(25). We tested whether HD3α could also physically interact with Akt by co-transfecting Flag-tagged HDAC3 and isoform plasmids together with HA-tagged Akt1 or Akt2 into 293 cells, followed by co-immunoprecipitation assays. HDAC3 and all four isoforms associated with Akt1 but not with Akt2 (Figure 5B). Further experiments revealed that HD3α associated with endogenous Akt1 in HAECs, and that this association was not affected by TGFβ1 (Figure 5C). Immuno-fluorescence staining confirmed the association of Akt1 and HD3α in HAECs, which did not seem to be affected by the presence of LY294002 (Figure 5D). As LY294002 is also reported to inhibit other signal pathways like Adamts1(39), the direct involvement of PI3K/Akt pathway in HD3α-driven EndMT was confirmed by siRNA-mediated knockdown assays. As shown in Figure 5E, knockdown of either PI3K p85alpha or Akt1 ablated Ad-HD3α-induced αSMA expression. However, HD3α-induced TGFβ2 secretion and cleavage seemed not affected. The deficiency of p85 and especially Akt1 significantly reduced HD3α protein level. These results suggest that PI3K/Akt1 may be not directly involved in TGFβ2 secretion and cleavage but are essential for HD3α-induced αSMA expression.

HD3α modulates HDAC3 functions

Being one of the isoforms, HD3α shares the same N-terminal and part of the internal sequence of fully-spliced HDAC3. Therefore, a natural question is whether HD3α can associate with and modulate HDAC3. Immunoprecipitation assay was first performed in 293 cells co-transfected with Flag-tagged HDAC3 and all four isoform plasmids together with HA-tagged HDAC3 plasmid. As expected, HDAC3 could form homodimer. HD3α, β and γ isoforms, but not HD3δ, could form heterodimer with HDAC3 (Figure 6A). Immunofluorescence staining with antibodies against the different C-terminal domains [Anti-HDAC3 (Sigma, H3034) against peptide from 411-428 amino acids of HDAC3 protein, and anti-HD3α raised against peptide derived from intron-12] confirmed the physical association of HDAC3 and HD3α, mainly in the cytoplasm (Figure 6B). Interestingly, HDAC3 protein levels in HD3α positive cells are much higher than that in HD3α negative cells, suggesting that HD3α may stabilize HDAC3. To test whether there is a crosstalk or interaction between HDAC3 and HD3α on EndMT, over-expression of HDAC3 via adenoviral transfer and suppression of HDAC3 activity via selective inhibitor apicidin(40) were included in Ad-HD3α-induced EndMT assays. Quantitative RT-PCR assays revealed that neither over-expression of HDAC3 nor inhibition of HDAC3 activity had significant effect on TGFβ2 and αSMA mRNA levels (Figure 6C). Over-expression of HDAC3 itself decreased basal level of EndMT phenotype as revealed by the decrease of αSMA, pSmad2 and Snail2 protein levels in cell lysate (Figure 6D) and decreased TGFβ2 secretion/activation in the medium (Figure 6E). In contrast, suppression of HDAC3 by

selective inhibitor apicidin induced TGFβ2 secretion/ activation and EndMT phenotype at basal levels and enhanced HD3α-induced EndMT (Figure 6D and 6E). A striking finding is that over-expression of HDAC3 enhances HD3α-induced TGFβ2 secretion although TGFβ2 cleavage (Figure 6E) and Smad2 phosphorylation and αSMA expression (Figure 6D) were suppressed when HDAC3 and HD3α are expressed together. Over-expression of HD3α increased endogenous and exogenous HDAC3 protein level, and over-expression of HDAC3 could also increase exogenous HD3α protein level (Figure 6D), confirming the immunefluorescence staining. These results suggest that HD3α may form a complex with HDAC3 and modulate HDAC3 function.

Discussion

EndMT is one type of EMT that refers only to vascular/cardiac endothelial cells undergoing mesenchymal transition, which contributes to cardiogenesis and a range of pathological fibrosis in human diseases(41-43). In the present study, we showed a novel finding that HDAC3 undergoes unconventional splicing to produce four different isoforms, of which HD3α contributes to stem cells differentiation and embryonic cardiovascular development. Over-expression of HD3α induces EndMT phenotype in mature ECs through TGFβ2 activation. These findings provide new insights into the mechanism of EndMT.

Unconventional splicing is a common event occurring in mammalian cells in different cellular processes, which makes it possible for a single gene to produce different proteins with different or even opposite functions. In this study, the occurrence of GFP in HD3α/β-GFP transfected cells, the specific band detected by Western blot and specific staining in mouse embryos with HD3α/β antibody have demonstrated that intron-12 is kept as an additional exon. In addition to intron-12 retaining, there seems recombination between exons as the spliced different exons cannot be produced from the routine splicing mechanisms. Due to the sequence differences in intron-12 among difference species, the HD3α isoform seems unique to the Mus Musculus. We have detected several isoforms from human HDAC3 (unpublished data), which are different from those HDAC3 isoforms in the Mus Musculus. Detailed investigations are still undergoing in deciphering how intron-12 is kept as an additional exon, how the recombination events occur and which human isoform possesses similar function as HD3α.

HDAC3 forms complex with co-repressors like N-CoR/SMRT and Ski, in which the co-repressors can activate HDAC3 deacetylase activity(44-46). These complexes may also contain other HDACs and suppress gene transcription via histone deacetylation. Structural analyses of HDAC3 protein indicate that the C-terminal domain is deacetylase catalytic domain and responsible for gene transcriptional repression, while the N-terminal domain is responsible for oligomerization of HDAC3 itself and interaction with other HDACs and proteins such as Akt1(25,47). In addition to its deacetylase activity, HDAC3 may function as a scaffold in complexes, in which the N-terminal domain plays an essential role(48,49). HD3α isoform retains the N-terminal domain. Therefore, it can form complex with HDAC3 protein. Indeed, we have detected the direct association of HD3α and HDAC3. The formation of the complex may modulate HDAC3 functions in several ways. First, HD3α may participate in HDAC3-complex. As the intron 12-derived C-terminal domain of HD3α is different from that of HDAC3, the involvement of HD3α in the complex may interfere with HDAC3 deacetylase activity, therefore attenuating the transcriptional repression effects. Secondly,

HD3α may compete with HDAC3 for binding to associated proteins, excluding HDAC3 from some complexes and ablating both the catalytic and scaffolding roles of HDAC3. It has been reported that HDAC3 can associate Akt and Smads(25,45). In our study, over-expression of HDAC3 decreases Smad2 phosphorylation, suggesting a suppressive role of HDAC3 in TGFβ signaling. As expected, we found the association of HD3α with Akt1 and Smad3. In contrast to suppressive effect of HDAC3 on Smad2 phosphorylation, HD3α increases Smad2 phosphorylation, suggesting that HD3α may interfere with HDAC3 interaction with Smad2 or modify the HDAC3/Smad2 complex. Further evidence on the competition hypothesis derives from the observation that over-expression of HD3α stabilizes HDAC3 protein. Immunofluorescence staining revealed that almost all HD3α proteins co-localize with HDAC3 and that the protein level of HDAC3 in HD3α-positive cells is much higher than that in HD3α-negative cells. When these two proteins were over-expressed together, the level of each protein is much higher than that in single over-expression system. The formation of HD3α/HDAC3 complex may prevent the association with degrading enzymes, therefore increasing the stabilization. The dimerization of HD3α and HDAC3 may also introduce HDAC3 into new signal pathways via the interaction of HD3α C-terminal domain with other proteins. Detailed investigation on the relationship between HD3α and HDAC3 is required.

Multiple factors have been reported to induce EndMT via several interactive signal pathways. The common factor is the TGFβ superfamily, in which TGFβ2 plays an indispensable role in EndMT *in vivo*(34). TGFβs bind to TGFβ type II receptor, which recruits and phosphorylates type I (ALK5) receptor. The latter activates Smad signaling pathways, leading to EndMT. In this study, we demonstrate that HD3α induces EndMT through TGFβ2. HD3α activates TGFβ2 in the extracellular matrix. The active TGFβ2 functions as an autocrine and paracrine factor to activate ALK5 receptor and Smad2/3 phosphorylation, leading to Snail2 up-regulation and EndMT. The evidence comes from the following observations. HD3α up-regulates Smad2/3 phosphorylation, and Snail2 and mesenchymal marker expression, which can be abolished by suppression of ALK5 receptor via SB435142. Higher amounts of cleaved TGFβ2 have been detected in conditioned medium from Ad-HD3α-infected HAECs as compared to Ad-null infected cells. Utilization of TGFβ2 neutralization antibody attenuates the HD3α-induced Smad2 phosphorylation and αSMA expression. Highly expressed αSMA was not only detected in HD3α positive cells but also in adjacent cells. High levels of active TGFβ2 were detected when SB435142 was present. SB431542 binds to ALK5, blocking downstream events. The binding of SB435142 to ALK5 may inhibit the binding of TGF β2 to type II receptor in a negative feedback mechanism, therefore accumulating TGFβ2 in the medium.

HD3α-induced activation of TGFβ2 occurs in the extracellular matrix via protease-mediated cleavage. TGFβs are secreted in a latent form, associating with latent TGFβs binding protein (LTBP)(50). Upon proteolytic cleavage, the LTBP and the latency associated peptide are removed from TGFβs molecules, giving rise to 13KD singlet or 25KD dimmer mature forms. Upon the over-expression of HD3α, no elevated TGFβs at mRNA and protein levels were discovered. However, the higher level of mature TGFβ2 was detected in Ad-HD3α-infected cell culture medium, suggesting that HD3α may activate certain proteases in the extracellular environment, whose expression and secretion were increased. Although TGFβ1 and TGFβ2 belong to the same family, their secretion mechanisms are different.

TGFβ1 is secreted via exosomes, while TGFβ2 seems not. Therefore, the extracellular location or binding partners will be different for TGFβ1 from TGFβ2, so is the activation mechanism involved, i.e. different proteases are responsible for the cleavage of TGFβ1 and TGFβ2. In this study, HD3α activates a few proteases, which locate in the cell surface or extracellular matrix but not in exosomes, therefore specifically initiate TGFβ2 cleavage but not TGFβ1

It has been reported that Smad-independent pathways are also involved in EndMT, such as MEK, PI3K/Akt, p38 and JNK MAP kinases, and G-proteins (Rho). In this study, we also discovered that the PI3K/Akt pathway is essential for HD3α-induced EndMT. However, it may not activate TGFβ2, as genetic knockdown of PI3K or Akt1 ablated HD3α-induced αSMA expression but did not affect TGFβ2 activation. In p85siRNA and Akt1 siRNA transfected cells, HD3α protein levels were significantly decreased, especially in the latter one. Akt1 binds to HD3α in the absence or presence of LY294002, indicating that Akt1 phosphorylation is not involved in the binding. The complex formation between Akt1 and HD3α may contribute to the stabilization of HD3α protein. Considering that LY294002 abolishes TGFβ2 activation, Smad phosphorylation and EndMT, while p85 or Akt1 knockdown does not affect TGFβ2 activation, it appears that other signal pathways may be involved, which is susceptible to LY294002.

In summary, HDAC3 mRNA undergoes unconventional splicing, in which intron-12 is kept as an additional exon and recombination occurs between exon 3 and exon 9, giving rise to HD3α isoform. The HD3α forms a complex with HDAC3 and Akt1 to promote TGFβ2 secretion and activation through a mechanism yet to be elucidated. The active TGFβ2 functions in an autocrine and paracrine manner to activate the ALK5-Smad2/3-Snail2 pathways, leading to EndMT (Figure 7). This study provides the first evidence that HDAC3 mRNA can undergo unconventional splicing to modulate HDAC3 and induce EndMT. Further detailed investigation on the mechanisms involved in HDAC3 splicing and how the isoforms exert their actions will undoubtedly contribute to further insights into the role of HDAC3 in the maintenance of endothelium integrity.

References

1. **Chi, J. T., Chang, H. Y., Haraldsen, G., Jahnsen, F. L., Troyanskaya, O. G., Chang, D. S., Wang, Z., Rockson, S. G., van de Rijn, M., Botstein, D., and Brown, P. O. (2003) Endothelial cell diversity revealed by global expression profiling. *Proc Natl Acad Sci U S A* 100, 10623-10628**
2. **Markwald, R. R., Fitzharris, T. P., and Smith, W. N. (1975) Sturctural analysis of endocardial cytodifferentiation. *Dev Biol* 42, 160-180**
3. **Markwald, R. R., Fitzharris, T. P., and Manasek, F. J. (1977) Structural development of endocardial cushions. *Am J Anat* 148, 85-119**
4. **Thiery, J. P., and Sleeman, J. P. (2006) Complex networks orchestrate epithelial-mesenchymal transitions. *Nat Rev Mol Cell Biol* 7, 131-142**
5. **Nakajima, Y., Yamagishi, T., Hokari, S., and Nakamura, H. (2000) Mechanisms involved in valvuloseptal endocardial cushion formation in early cardiogenesis: roles of transforming growth factor (TGF)-beta and bone morphogenetic protein (BMP). *The Anatomical record* 258, 119-127**
6. **Wang, J., Sridurongrit, S., Dudas, M., Thomas, P., Nagy, A., Schneider, M. D., Epstein, J.**

A., and Kaartinen, V. (2005) Atrioventricular cushion transformation is mediated by ALK2 in the developing mouse heart. *Dev Biol* 286, 299-310

7. Armulik, A., Abramsson, A., and Betsholtz, C. (2005) Endothelial/pericyte interactions. *Circ Res* 97, 512-523
8. Zeisberg, E. M., Tarnavski, O., Zeisberg, M., Dorfman, A. L., McMullen, J. R., Gustafsson, E., Chandraker, A., Yuan, X., Pu, W. T., Roberts, A. B., Neilson, E. G., Sayegh, M. H., Izumo, S., and Kalluri, R. (2007) Endothelial-to-mesenchymal transition contributes to cardiac fibrosis. *Nat Med* 13, 952-961
9. Zeisberg, E. M., Potenta, S. E., Sugimoto, H., Zeisberg, M., and Kalluri, R. (2008) Fibroblasts in kidney fibrosis emerge via endothelial-to-mesenchymal transition. *J Am Soc Nephrol* 19, 2282-2287
10. Arciniegas, E., Frid, M. G., Douglas, I. S., and Stenmark, K. R. (2007) Perspectives on endothelial-to-mesenchymal transition: potential contribution to vascular remodeling in chronic pulmonary hypertension. *Am J Physiol Lung Cell Mol Physiol* 293, L1-8
11. Potenta, S., Zeisberg, E., and Kalluri, R. (2008) The role of endothelial-to-mesenchymal transition in cancer progression. *Br J Cancer* 99, 1375-1379
12. Zeisberg, E. M., Potenta, S., Xie, L., Zeisberg, M., and Kalluri, R. (2007) Discovery of endothelial to mesenchymal transition as a source for carcinoma-associated fibroblasts. *Cancer Res* 67, 10123-10128
13. Potts, J. D., and Runyan, R. B. (1989) Epithelial-mesenchymal cell transformation in the embryonic heart can be mediated, in part, by transforming growth factor beta. *Dev Biol* 134, 392-401
14. Armstrong, E. J., and Bischoff, J. (2004) Heart valve development: endothelial cell signaling and differentiation. *Circ Res* 95, 459-470
15. Meadows, K. N., Iyer, S., Stevens, M. V., Wang, D., Shechter, S., Perruzzi, C., Camenisch, T. D., and Benjamin, L. E. (2009) Akt promotes endocardial-mesenchyme transition. *Journal of angiogenesis research* 1, 2
16. Chen, P. Y., Qin, L., Barnes, C., Charisse, K., Yi, T., Zhang, X., Ali, R., Medina, P. P., Yu, J., Slack, F. J., Anderson, D. G., Kotelianski, V., Wang, F., Tellides, G., and Simons, M. (2012) FGF Regulates TGF-beta Signaling and Endothelial-to-Mesenchymal Transition via Control of let-7 miRNA Expression. *Cell reports* 2, 1684-1696
17. de Ruijter, A. J., van Gennip, A. H., Caron, H. N., Kemp, S., and van Kuilenburg, A. B. (2003) Histone deacetylases (HDACs): characterization of the classical HDAC family. *Biochem J* 370, 737-749
18. Gallinari, P., Di Marco, S., Jones, P., Pallaoro, M., and Steinkuhler, C. (2007) HDACs, histone deacetylation and gene transcription: from molecular biology to cancer therapeutics. *Cell Res* 17, 195-211
19. Kekatpure, V. D., Dannenberg, A. J., and Subbaramaiah, K. (2009) HDAC6 modulates Hsp90 chaperone activity and regulates activation of aryl hydrocarbon receptor signaling. *J Biol Chem* 284, 7436-7445
20. Zilberman, Y., Ballestrem, C., Carramusa, L., Mazitschek, R., Khochbin, S., and Bershadsky, A. (2009) Regulation of microtubule dynamics by inhibition of the tubulin deacetylase HDAC6. *J Cell Sci* 122, 3531-3541
21. Margariti, A., Xiao, Q., Zampetaki, A., Zhang, Z., Li, H., Martin, D., Hu, Y., Zeng, L.,

and Xu, Q. (2009) Splicing of HDAC7 modulates the SRF-myocardin complex during stem-cell differentiation towards smooth muscle cells. *J Cell Sci* 122, 460-470

22. **Margariti, A., Zampetaki, A., Xiao, Q., Zhou, B., Karamariti, E., Martin, D., Yin, X., Mayr, M., Li, H., Zhang, Z., De Falco, E., Hu, Y., Cockerill, G., Xu, Q., and Zeng, L. (2010) Histone Deacetylase 7 Controls Endothelial Cell Growth Through Modulation of {beta}-Catenin. *Circ Res* 106:1202-11**
23. **Emiliani, S., Fischle, W., Van Lint, C., Al-Abed, Y., and Verdin, E. (1998) Characterization of a human RPD3 ortholog, HDAC3. *Proc Natl Acad Sci U S A* 95, 2795-2800**
24. **Bhaskara, S., Chyla, B. J., Amann, J. M., Knutson, S. K., Cortez, D., Sun, Z. W., and Hiebert, S. W. (2008) Deletion of histone deacetylase 3 reveals critical roles in S phase progression and DNA damage control. *Mol Cell* 30, 61-72**
25. **Zampetaki, A., Zeng, L., Margariti, A., Xiao, Q., Li, H., Zhang, Z., Pepe, A. E., Wang, G., Habi, O., deFalco, E., Cockerill, G., Mason, J. C., Hu, Y., and Xu, Q. (2010) Histone deacetylase 3 is critical in endothelial survival and atherosclerosis development in response to disturbed flow. *Circulation* 121, 132-142**
26. **Zeng, L., Xiao, Q., Margariti, A., Zhang, Z., Zampetaki, A., Patel, S., Capogrossi, M. C., Hu, Y., and Xu, Q. (2006) HDAC3 is crucial in shear- and VEGF-induced stem cell differentiation toward endothelial cells. *J Cell Biol* 174, 1059-1069**
27. **Xiao, Q., Zeng, L., Zhang, Z., Margariti, A., Ali, Z. A., Channon, K. M., Xu, Q., and Hu, Y. (2006) Sca-1+ progenitors derived from embryonic stem cells differentiate into endothelial cells capable of vascular repair after arterial injury. *Arterioscler Thromb Vasc Biol* 26, 2244-2251**
28. **Zeng, L., Zampetaki, A., Margariti, A., Pepe, A. E., Alam, S., Martin, D., Xiao, Q., Wang, W., Jin, Z. G., Cockerill, G., Mori, K., Li, Y. S., Hu, Y., Chien, S., and Xu, Q. (2009) Sustained activation of XBP1 splicing leads to endothelial apoptosis and atherosclerosis development in response to disturbed flow. *Proc Natl Acad Sci U S A* 106, 8326-8331**
29. **Kumarswamy, R., Volkmann, I., Jazbutyte, V., Dangwal, S., Park, D. H., and Thum, T. (2012) Transforming growth factor-beta-induced endothelial-to-mesenchymal transition is partly mediated by microRNA-21. *Arterioscler Thromb Vasc Biol* 32, 361-369**
30. **Mihira, H., Suzuki, H. I., Akatsu, Y., Yoshimatsu, Y., Igarashi, T., Miyazono, K., and Watabe, T. (2012) TGF-beta-induced mesenchymal transition of MS-1 endothelial cells requires Smad-dependent cooperative activation of Rho signals and MRTF-A. *J Biochem* 151, 145-156**
31. **Medici, D., Potenta, S., and Kalluri, R. (2011) Transforming growth factor-beta2 promotes Snail-mediated endothelial-mesenchymal transition through convergence of Smad-dependent and Smad-independent signalling. *Biochem J* 437, 515-520**
32. **Wang, J., Kuiatse, I., Lee, A. V., Pan, J., Giuliano, A., and Cui, X. (2010) Sustained c-Jun-NH2-kinase activity promotes epithelial-mesenchymal transition, invasion, and survival of breast cancer cells by regulating extracellular signal-regulated kinase activation. *Mol Cancer Res* 8, 266-277**
33. **Derynck, R., and Zhang, Y. E. (2003) Smad-dependent and Smad-independent pathways in TGF-beta family signalling. *Nature* 425, 577-584**
34. **Azhar, M., Runyan, R. B., Gard, C., Sanford, L. P., Miller, M. L., Andringa, A.,**

Pawlowski, S., Rajan, S., and Doetschman, T. (2009) Ligand-specific function of transforming growth factor beta in epithelial-mesenchymal transition in heart development. *Dev Dyn* 238, 431-442

35. **Schniewind, B., Groth, S., Sebens Muerkoster, S., Sipos, B., Schafer, H., Kalthoff, H., Fandrich, F., and Ungefroren, H. (2007) Dissecting the role of TGF-beta type I receptor/ALK5 in pancreatic ductal adenocarcinoma: Smad activation is crucial for both the tumor suppressive and prometastatic function. *Oncogene* 26, 4850-4862**
36. **Clayton, A., Mitchell, J. P., Court, J., Mason, M. D., and Tabi, Z. (2007) Human tumor-derived exosomes selectively impair lymphocyte responses to interleukin-2. *Cancer Res* 67, 7458-7466**
37. **Thery, C., Regnault, A., Garin, J., Wolfers, J., Zitvogel, L., Ricciardi-Castagnoli, P., Raposo, G., and Amigorena, S. (1999) Molecular characterization of dendritic cell-derived exosomes. Selective accumulation of the heat shock protein hsc73. *J Cell Biol* 147, 599-610**
38. **Larue, L., and Bellacosa, A. (2005) Epithelial-mesenchymal transition in development and cancer: role of phosphatidylinositol 3' kinase/AKT pathways. *Oncogene* 24, 7443-7454**
39. **Hatipoglu, O. F., Hirohata, S., Cilek, M. Z., Ogawa, H., Miyoshi, T., Obika, M., Demircan, K., Shinohata, R., Kusachi, S., and Ninomiya, Y. (2009) ADAMTS1 is a unique hypoxic early response gene expressed by endothelial cells. *J Biol Chem* 284, 16325-16333**
40. **Strobl, J. S., Cassell, M., Mitchell, S. M., Reilly, C. M., and Lindsay, D. S. (2007) Scriptaid and suberoylanilide hydroxamic acid are histone deacetylase inhibitors with potent anti-Toxoplasma gondii activity in vitro. *J Parasitol* 93, 694-700**
41. **Piera-Velazquez, S., Li, Z., and Jimenez, S. A. (2011) Role of endothelial-mesenchymal transition (EndoMT) in the pathogenesis of fibrotic disorders. *Am J Pathol* 179, 1074-1080**
42. **Chang, A. C., Fu, Y., Garside, V. C., Niessen, K., Chang, L., Fuller, M., Setiadi, A., Smrz, J., Kyle, A., Minchinton, A., Marra, M., Hoodless, P. A., and Karsan, A. (2011) Notch Initiates the Endothelial-to-Mesenchymal Transition in the Atrioventricular Canal through Autocrine Activation of Soluble Guanylyl Cyclase. *Dev Cell* 21, 288-300**
43. **Aisagbonhi, O., Rai, M., Ryzhov, S., Atria, N., Feoktistov, I., and Hatzopoulos, A. K. (2011) Experimental myocardial infarction triggers canonical Wnt signaling and endothelial-to-mesenchymal transition. *Dis Model Mech* 4, 469-483**
44. **Li, J., Wang, J., Wang, J., Nawaz, Z., Liu, J. M., Qin, J., and Wong, J. (2000) Both corepressor proteins SMRT and N-CoR exist in large protein complexes containing HDAC3. *EMBO J* 19, 4342-4350**
45. **Tabata, T., Kokura, K., Ten Dijke, P., and Ishii, S. (2009) Ski co-repressor complexes maintain the basal repressed state of the TGF-beta target gene, SMAD7, via HDAC3 and PRMT5. *Genes Cells* 14, 17-28**
46. **Guenther, M. G., Barak, O., and Lazar, M. A. (2001) The SMRT and N-CoR corepressors are activating cofactors for histone deacetylase 3. *Mol Cell Biol* 21, 6091-6101**
47. **Yang, W. M., Tsai, S. C., Wen, Y. D., Fejer, G., and Seto, E. (2002) Functional domains of histone deacetylase-3. *J Biol Chem* 277, 9447-9454**

48. **Alam, S., Li, H., Margariti, A., Martin, D., Zampetaki, A., Habi, O., Cockerill, G., Hu, Y., Xu, Q., and Zeng, L. (2011) Galectin-9 protein expression in endothelial cells is positively regulated by histone deacetylase 3. *J Biol Chem* 286, 44211-44217**

49. **Togi, S., Kamitani, S., Kawakami, S., Ikeda, O., Muromoto, R., Nanbo, A., and Matsuda, T. (2009) HDAC3 influences phosphorylation of STAT3 at serine 727 by interacting with PP2A. *Biochem Biophys Res Commun* 379, 616-620**

50. **Miyazono, K., Olofsson, A., Colosetti, P., and Heldin, C. H. (1991) A role of the latent TGF-beta 1-binding protein in the assembly and secretion of TGF-beta 1. *EMBO J* 10, 1091-1101**

Acknowledgement

This work was supported by Grants from British Heart Foundation, the Oak Foundation and National Natural Science Foundation of China (81300116).

Declaration

None of the authors has conflicts of interest.

Figure Legends

Figure 1: HDAC3 undergoes unconventional splicing. (A-C) Multiple bands of HDAC3 were detected in differentiated embryonic stem (DES) cells (A), mouse embryos (B) and adult tissues (C). Undifferentiated ES cells (ES) were included as control cells, and β-actin was included as loading control. (D) Schematic illustration of the sequence structure of cloned HDAC3 and splicing variants. The open box stands for exon with number inside; The shadowed box is for intron-12; The length of each isoform was labeled at the DNA base (bp) and amino acid (aa) levels; The taa or tag is stop codon. The stretched box indicates the Flag tag. Arrows indicate the primer positions. (E) Western blot showed the protein bands for HDAC3 and the splicing isoforms in transfected 293 cells. (F) & (G) HDAC3 splicing occurred naturally during stem cell differentiation as revealed by GFP observation (F) and Western blot (G). (F) HD3α/β-GFP knock-in (upper schematic illustration) ES cells were cultured in collagen I-coated flask in differentiation medium for 3 days, followed by imaging at inverted phase (left) and fluorescence (right) microscopes. (G) ES cells were cultured in collagen I-coated flask in differentiation medium for 2 days followed by treatment with 10ng/ml rat PDGF-BB, 5ng/ml TGFβ1 or 5ng/ml VEGF. Western blot analysis was performed with anti-HD3α antibody pretreated with (right)/without (left) blocking peptide. Cell lysates from 293 cell transfected with pShuttle2-Flag-HD3α (HD3α/293) and pShuttle2-Flag-HD3β (HD3β/293) were included as positive control. (H) & (I) quantitative RT-PCR analysis of the effect of over-expression of HD3α on VE-Cad and SM22 expression in ES (E) and ES-derived EC (F) differentiation. *: $p<0.05$; **: $p<0.01$. Data presented are representative or average of three independent experiments.

Figure 2 HDAC3 splicing may contribute to mouse embryonic development. (A) HD3α co-localized with CD31 at 10.5dpc stage. Triple staining for DAPI (blue), CD31 (red) and HD3α (green) was performed on mouse 10.5dpc sections in the presence (a) or absence of HD3α blocking peptide. (c) Higher magnificence shows the co-localization of HD3α and CD31. (B) HD3α co-localized with αSMA (b) but not with CD31 (a) at 12.5dpc stage. Triple staining for DAPI (blue),

CD31 (red, a)/ αSMA (red, b) and HD3α (green) was performed on mouse 12.5dpc sections. (c) Higher magnificence shows the co-localization of HD3α and αSMA. Data shown are representatives for at least three independent experiments.

Figure 3: Over-expression of HD3α induces EndMT via PI3K/Akt and TGFβ signal pathways. (A) Over-expression of HD3α induced cell morphology change in HAECs. Images were taken at day 5 post infection. (B) Over-expression of HD3α induced EndMT phenotype in a dose dependent manner as revealed by the decrease of CD31 and the increase of mesenchymal markers. (C) Immunofluorescence staining revealed that over-expression of HD3α induced the redistribution of VE-cad (green) in HD3α-positive cells (Flag, red; arrowhead), and the expression of αSMA (red) in HD3α-positive cells (Flag, green; arrow) and adjacent cells. (D) PI3K-Akt and TGFβ signal pathways were essential for HD3α-induced αSMA expression in HAECs. Inhibitors LY294002 ($5x10^{-6}$mol/L), PD98059 ($1x10^{-5}$mol/L), SB431542 ($1x10^{-5}$mol/L), SB202190 ($1x10^{-5}$mol/L), SP6005 ($1x10^{-5}$mol/L) and Y27632 ($1x10^{-5}$mol/L) were included in virus infection (10MOI, 6hr) and incubation in SFM (24hr). Ad-null was included as virus control, and DMSO was included as vehicle control. Flag antibody was used to detect exogenous HD3α. (E) Both LY294002 and SB431542 abolished Ad-HD3α-induced EndMT. $5x10^{-6}$mol/L of LY294002 or $1x10^{-5}$mol/L SB431542 was included in virus infection (10 MOI for 6hr) and further incubation in M199 medium supplemented with 1% FBS. Immunofluorescence staining was performed to detect VE-Cad (red) and αSMA (green) at day 5 post infection. DMSO was included as vehicle control. Data presented are representatives of three independent experiments.

Figure 4: Over-expression of HD3α induces EndMT through TGFβ2 secretion and activation. (A) Over-expression of HD3α activated TGFβ signaling pathway. Tubulin and histone H4 were used to indicate cytosol and nuclear extract fractions, respectively. (B) TGFβ1 enhanced HD3α-induced EndMT. Ad-null or Ad-HD3α infected HAECs were treated with 5ng/ml of TGFβ1 or TGFβ2 in serum free medium for 24hr, followed by Western blot analysis. Numbers are relative amounts of phosphor-Smad2 averaged from three independent experiments. (C) Over-expression of HD3α enhanced TGFβ1-induced Smad2 phosphorylation (green) and nuclear translocation. Flag antibody was used to identify exogenous HD3α (red). (D) Over-expression of HD3α did not affect TGFβs mRNA levels. (E-G) LY294002 abolished Ad-HD3α-induced TGFβ2 activation and Smad2 phosphorylation. $5x10^{-6}$mol/L LY294002 or $1x10^{-5}$mol/L SB431542 was included in virus infection (10MOI for 6hr) and incubation process (M199 supplemented with 5ng/ml insulin for 24hr), followed by Western blot analysis (without 2-mercaptoethanol) of cell lysates (E) and conditioned media (F and G). DMSO was included as vehicle control. *: $p<0.05$; **: $p<0.01$. (H) TGFβ2 did not exist in exosomes. Ad-null or Ad-HD3α-infected HAECs were incubated with serum free medium containing 5ng/ml insulin for 24hr, followed by Western blot analysis (with 2-mercaptoethanol) of cell lysate (Lys, 25μg protein), exosomes (EM, from 1ml medium/lane) and whole medium concentrates (MC, from 1ml/lane). CD9 was used to indicate exosomes. Arrow indicates the 13KD active band. (I) TGFβ2 neutralization antibody attenuated HD3α-induced Smad2 phosphorylation and αSMA expression. For all Western blot analyses, Flag antibody was used to detect exogenous HD3α, while GAPDH was included as loading control. Data are representative or averages of three independent experiments.

Figure 5: HD3α physically interacts with Akt1. (A) HD3α did not activate Akt phosphorylation.

Flag antibody was used to detect exogenous HD3α, GAPDH was included as loading control. (B) Western blot detected the association of HDAC3 and its isoforms with Akt1. 293 cells were transfected with Flag-HDAC3, Flag-HD3α,β,γ,δ together with HA-Akt1 or HA-Akt2, followed by immunoprecipitation with anti-HA antibody and Western blot with anti-Flag and HA antibodies. (C) TGFβ1 enhanced HD3α association with Smad3 but did not affect HD3α association with Akt1. (D) LY294002 did not affect the association of HD3α with Akt1. HAECs were infected with Ad-HD3α at 10 MOI in the presence of DMSO or $5x10^{-6}$mol/L LY294002 for 6hr and then cultured in serum free medium in the presence of DMSO or LY294002 for 24hr, followed by immunofluorescence staining with anti-Akt1 (green) and Flag (red) antibodies. (E) PI3K and Akt1 were essential for HD3α-induced αSMA expression. HAECs were transfected with p85siRNA or Akt1 siRNA for 48hr, followed by Ad- HD3α infection for 48hr. Prior to harvesting cell lysate and culture medium, the cells were treated with serum free M199 for 24hr. Data presented are representatives of three independent experiments.

Figure 6: HD3α modulates HDAC3 function. (A) Western blot analysis detected the association of HDAC3 isoforms with HDAC3 in HEK293 cells. All isoforms except HD3δ associated with HDAC3. (B) HD3α physically associated with and stabilized HDAC3. HAECs were infected with Ad-HD3α at 10 MOI for 6hr in complete growth medium and cultured in serum free medium for 24hr, followed by immunofluorescence staining with anti-HDAC3 (green) and anti-Flag (for HD3α, red). (C-E) Effect of over-expression or suppression of HDAC3 on HD3α-induced EndMT. HAECs were co-infected with Ad-HD3α (10 MOI) and Ad-HDAC3 (10 MOI) or in the presence of $1x10^{-5}$mol/L apicidin in complete growth medium for 6hr, then cultured in M199 medium supplemented with 5ng/ml insulin for 24hr, followed by (C) quantitative RT-PCR analysis of TGFβ2 and αSMA mRNA levels, (D) Western blot analysis of cell lysates, and (E) Western blot analysis of conditioned media with the ratio of cleaved to precursor TGFβ2 indicated in the lower panel. Ad-null is included as control and to normalize variations in MOI. DMSO was included as vehicle control. *: $p<0.05$; **: $p<0.01$. Data presented are representatives or average of three independent experiments.

Figure 7: Schematic illustration of HDAC3 splicing-induced EndMT. Upon some kinds of stimuli, HDAC3 mRNA undergoes unconventional splicing *(1)*, in which intron-12 is kept as an additional exon and recombination occurs between exon 3 and exon 9, giving rise to HD3α isoform. The HD3α forms a complex with HDAC3 and Akt1 *(2)*, which in turn promote TGFβ2 secretion and activation through unknown mechanisms *(3)*. The active TGFβ2 functions in an autocrine and paracrine manner to activate Alk5-Smad2/3-Snail2 pathways *(4,5)*, leading to EndMT.

Figure 1

Zeng L et al

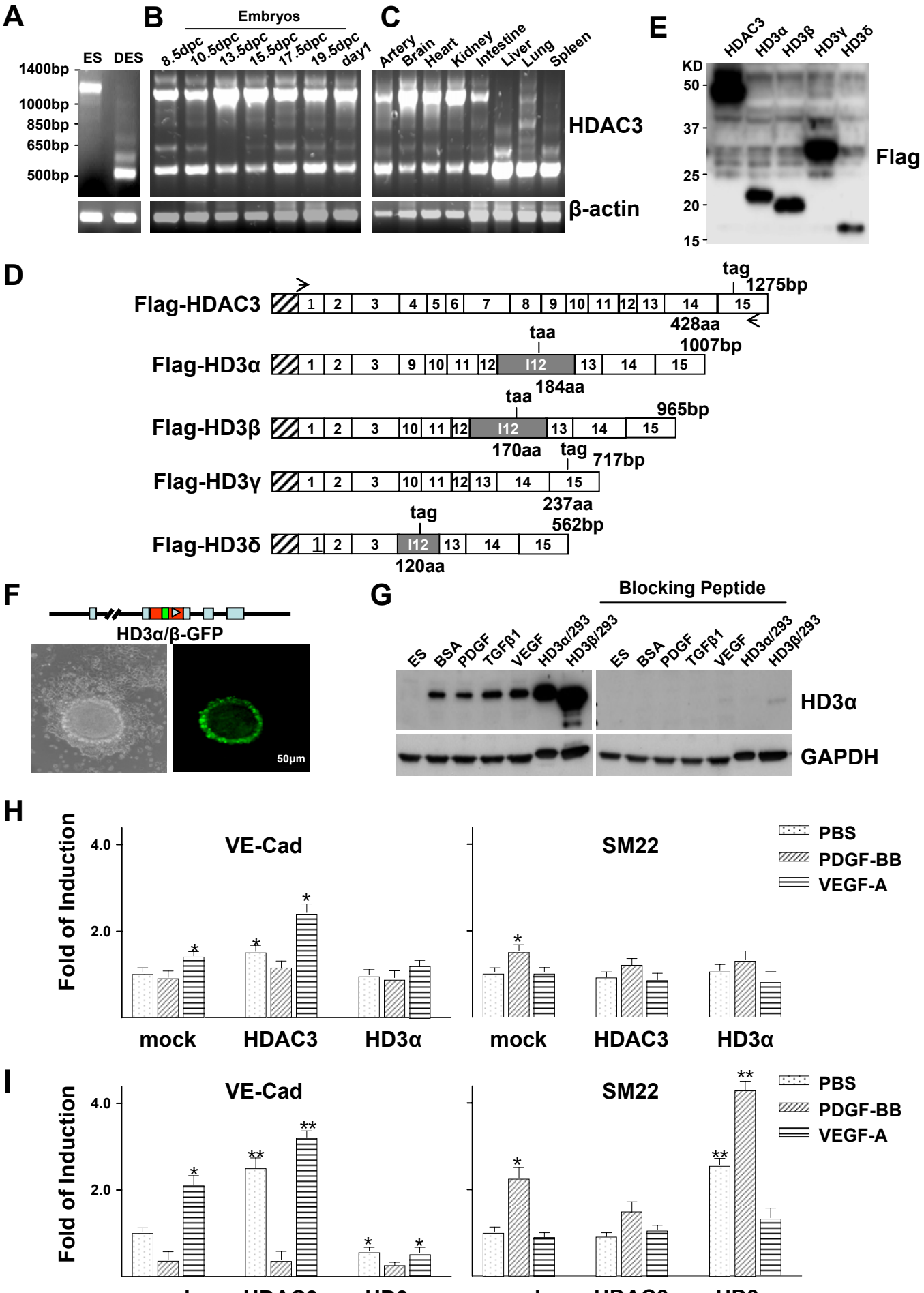

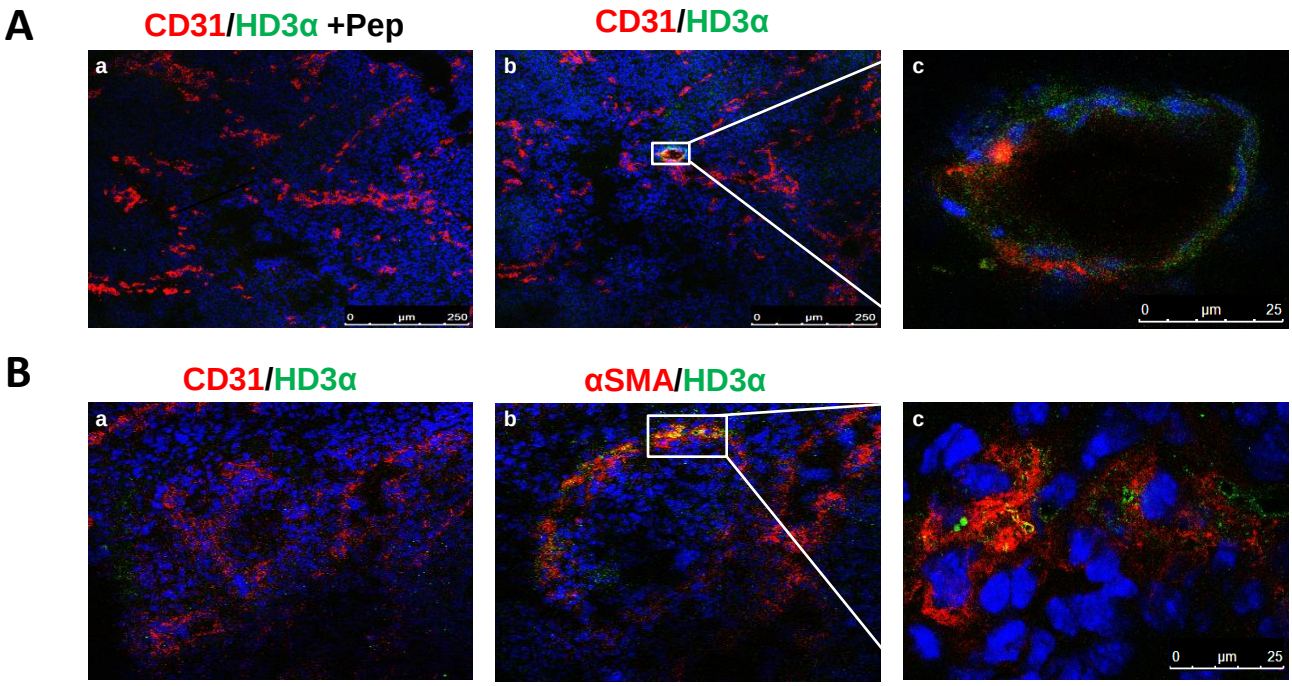
A
CD31/HD3α +Pep
CD31/HD3α
a
b
c
0 μm 250
0 μm 250
0 μm 25
B
CD31/HD3α
αSMA/HD3α
a
b
c
0 μm 25

Figure 3

Zeng L et al

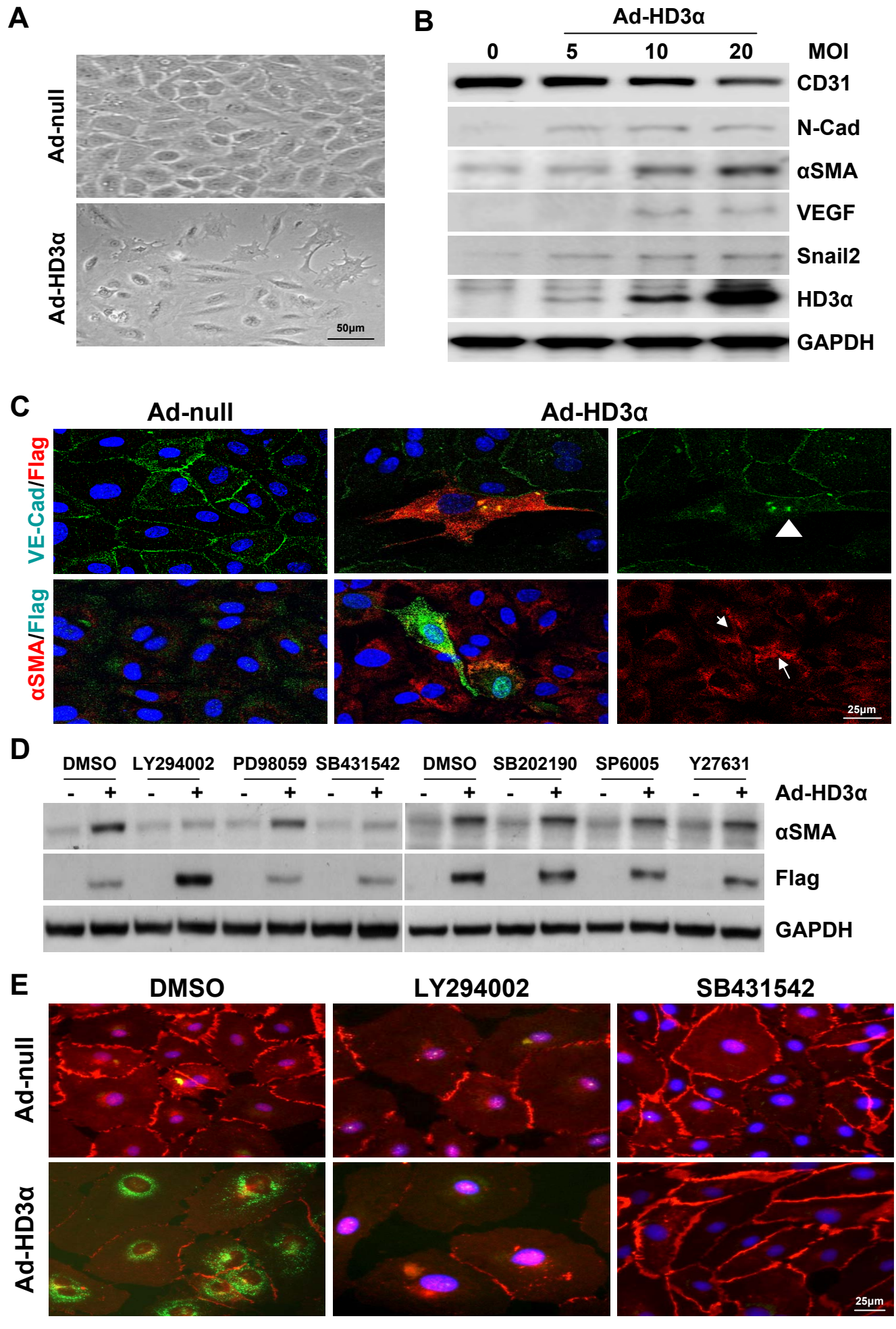

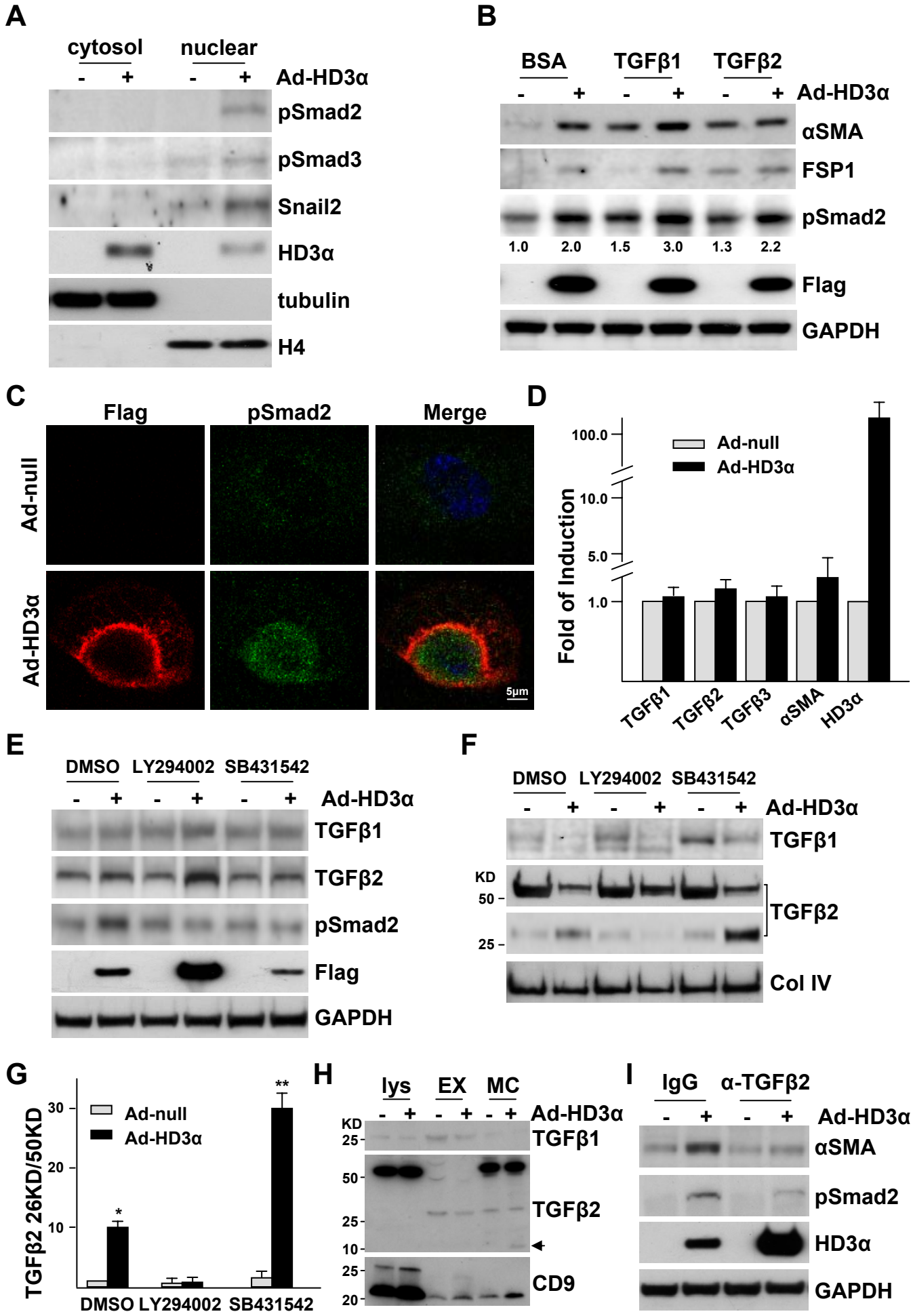
A
cytosol
nuclear
- + - +
Ad-HD3α
pSmad2
pSmad3
Snail2
HD3α
tubulin
H4
B
BSA
TGFβ1
TGFβ2
- + - + - +
Ad-HD3α
αSMA
FSP1
pSmad2
1.0 2.0 1.5 3.0 1.3 2.2
Flag
GAPDH
C
Flag
pSmad2
Merge
Ad-null
Ad-HD3α
5μm
D
Ad-null
Ad-HD3α
Fold of Induction
100.0
10.0
5.0
1.0
TGFβ1
TGFβ2
TGFβ3
αSMA
HD3α
E
DMSO
LY294002
SB431542
- + - + - +
Ad-HD3α
TGFβ1
TGFβ2
pSmad2
Flag
GAPDH
F
DMSO
LY294002
SB431542
- + - + - +
Ad-HD3α
TGFβ1
KD
50
25
TGFβ2
Col IV
G
Ad-null
Ad-HD3α
TGFβ2 26KD/50KD
30
20
10
*
**
DMSO LY294002 SB431542
H
lys
EX
MC
- + - + - +
Ad-HD3α
KD
25
TGFβ1
50
25
10
TGFβ2
25
20
CD9
I
IgG
α-TGFβ2
- + - +
Ad-HD3α
αSMA
pSmad2
HD3α
GAPDH

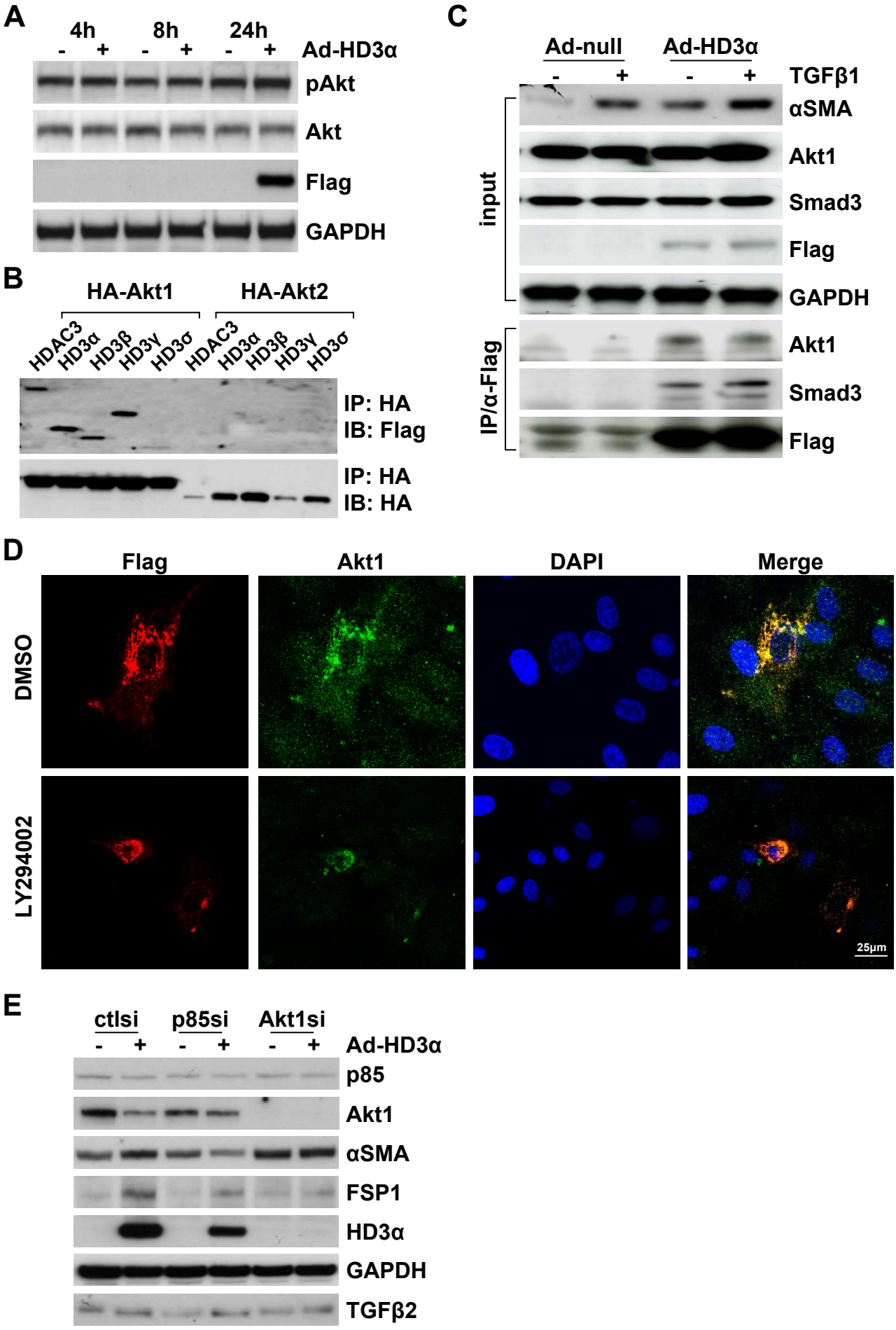
A
4h
8h
24h
- + - + - +
Ad-HD3α
pAkt
Akt
Flag
GAPDH
B
HA-Akt1
HA-Akt2
HDAC3
HD3α
HD3β
HD3γ
HD3σ
IP: HA
IB: Flag
IP: HA
IB: HA
C
Ad-null
Ad-HD3α
- + - +
TGFβ1
αSMA
Akt1
Smad3
Flag
GAPDH
input
IP/α-Flag
Akt1
Smad3
Flag
D
Flag
Akt1
DAPI
Merge
DMSO
LY294002
25μm
E
ctlsi
p85si
Akt1si
- + - + - +
Ad-HD3α
p85
Akt1
αSMA
FSP1
HD3α
GAPDH
TGFβ2

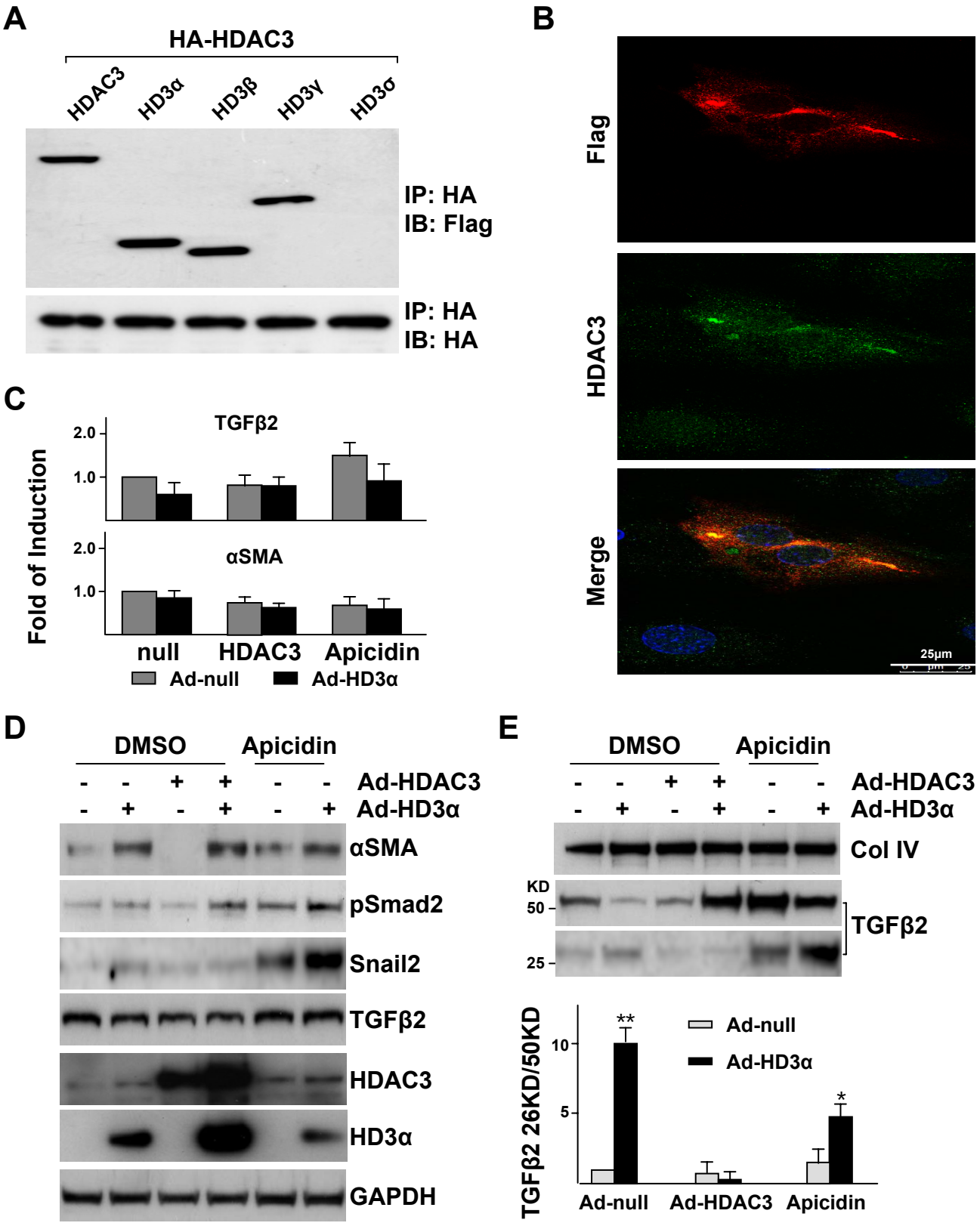
A
HA-HDAC3
HDAC3
HD3α
HD3β
HD3γ
HD3σ
IP: HA
IB: Flag
IP: HA
IB: HA
B
Flag
HDAC3
Merge
25μm
C
TGFβ2
αSMA
Fold of Induction
2.0
1.0
null
HDAC3
Apicidin
Ad-null
Ad-HD3α
D
DMSO
Apicidin
Ad-HDAC3
Ad-HD3α
αSMA
pSmad2
Snail2
TGFβ2
HDAC3
HD3α
GAPDH
E
DMSO
Apicidin
Ad-HDAC3
Ad-HD3α
Col IV
KD
50
25
TGFβ2
TGFβ2 26KD/50KD
10
5
**
*
Ad-null
Ad-HD3α
Ad-null
Ad-HDAC3
Apicidin

Figure 7

Zeng L et al